

# Crystallisation of Lithium Magnesium Zinc Silicates

## Part 1 *Phase Equilibria in the System*



A. R. WEST, F. P. GLASSER

*Department of Chemistry, University of Aberdeen, Old Aberdeen, Scotland*

The  $\text{Li}_4\text{SiO}_4\text{--Mg}_2\text{SiO}_4$  binary system contains a congruently-melting phase,  $\text{Li}_2\text{MgSiO}_4$ , which has an  $\text{Li}_3\text{PO}_4$ -type structure and is isostructural with  $\text{Li}_2\text{ZnSiO}_4$  at high temperatures.  $\text{Li}_2\text{MgSiO}_4$  and  $\text{Li}_4\text{SiO}_4$  exhibit considerable mutual solubility. Slow cooling of their solid solutions causes some exsolution and both phases undergo a series of transformations. More rapid quenching, followed by annealing at lower temperatures, gives rise to several metastable orthosilicate phases. The binary join  $\text{Li}_2\text{MgSiO}_4\text{--Li}_2\text{ZnSiO}_4$  shows complete solid solution in the  $\gamma$ -phase above  $870^\circ\text{C}$ . At lower temperatures, a wide range of compositions, from 0 to  $\sim 80\%$   $\text{Li}_2\text{MgSiO}_4$ , transforms to a  $\beta$ -phase. Ternary isothermal sections are shown at 1200, 900 and  $700^\circ\text{C}$ . These have extensive areas of  $\text{Li}_4\text{SiO}_4$ -type and  $\text{Li}_2(\text{Zn, Mg})\text{SiO}_4$ -type solid solution.  $\text{Li}_4\text{SiO}_4$  does not dissolve in either olivine or willemite solid solutions to any appreciable extent.

### 1. Introduction

Crystallisation of silicate glasses yields a useful new class of materials: glass-ceramics. In the crystallisation stage both stable and metastable phases may form. Our knowledge of the relevant phase compositions and equilibria are often outstripped by the empirical development of new glass-ceramic compositions. However, their development has created new interest in the nature of the crystallisation processes and in processes which may precede crystallisation, such as amorphous phase separation. Compositions which are based on the  $\text{Li}_2\text{O--SiO}_2$  or on the  $\text{ZnO--SiO}_2$  systems are known to yield useful glass-ceramics, although, of course most practical glass-ceramics are chemically much more complex. Again, development of these compositions has proceeded along largely empirical lines. Our attention was directed towards the  $\text{Li}_2\text{O--ZnO--SiO}_2$  system because, in a search for simple "model" systems, crystallisation studies on  $\text{Li}_2\text{O--SiO}_2$  glasses and undercooled melts [1, 2], and on  $\text{ZnO--SiO}_2$  glasses [3] had previously been undertaken. Also glass-ceramics made from  $\text{Li}_2\text{O--ZnO--SiO}_2$  compositions containing only small amounts of  $\text{K}_2\text{O}$  and  $\text{P}_2\text{O}_5$  have been described [4, 5].

In an effort to increase the relevance of our studies to the chemically more complex commercial glass-ceramics, a number of  $\text{Li}_2\text{O--ZnO--SiO}_2$  compositions had been melted, quenched to glasses and subsequently devitrified. Our inability to explain the variation in the physical properties of the orthosilicate phases lead, in turn, to a more thorough study of the stable and metastable phase relations in the system  $\text{Li}_4\text{SiO}_4\text{--Zn}_2\text{SiO}_4$ . It is an unusual property of melts in the  $\text{Li}_2\text{O--ZnO--SiO}_2$  system that an orthosilicate phase can be crystallised from a wide range of compositions, including many in the glass-forming region. Hence the importance of the orthosilicate phase. These studies [6, 7] disclosed a number of unusual features. Extensive solid solution occurs between several of the orthosilicates, despite the difference in charge between  $\text{Li}^+$  and  $\text{Zn}^{2+}$ . The polymorphism of  $\text{Li}_2\text{ZnSiO}_4$  proved to be unexpectedly complex; seven polymorphs could be prepared. These polymorphs are structurally related and belong to the  $\text{Li}_3\text{PO}_4$  family. Finally, phase transformations could be effected in reasonable times even at temperatures as low as  $300^\circ\text{C}$ , although the transformations were often metastable.

The present studies are aimed at finding out if

similar phenomena will occur in systems of greater chemical complexity, and demonstrating that such systems can be accurately and rapidly explored. First, data are presented for the system  $\text{Li}_4\text{SiO}_4\text{-Mg}_2\text{SiO}_4$  and compared with those obtained for the  $\text{Li}_4\text{SiO}_4\text{-Zn}_2\text{SiO}_4$  system. From this comparison, equilibria may be predicted for the ternary system of the three orthosilicates:  $\text{Li}_4\text{SiO}_4\text{-Zn}_2\text{SiO}_4\text{-Mg}_2\text{SiO}_4$ . Three ternary isothermal sections have been studied experimentally; these data are presented.

In Part 2, phase distributions in the  $\text{Li}_2\text{O-ZnO-SiO}_2$  system are explored at 650 and 900°C. Further data are presented to show compatibility relationships in the  $\text{SiO}_2$ -rich portions of the quaternary system  $\text{Li}_2\text{O-MgO-ZnO-SiO}_2$  including those which are likely to be observed under both equilibrium and non-equilibrium conditions. Physical properties, including solubilities, are given for some of the orthosilicate phases.

## 2. Experimental

The experimental techniques are similar to those used in previous studies [6, 7]. The same

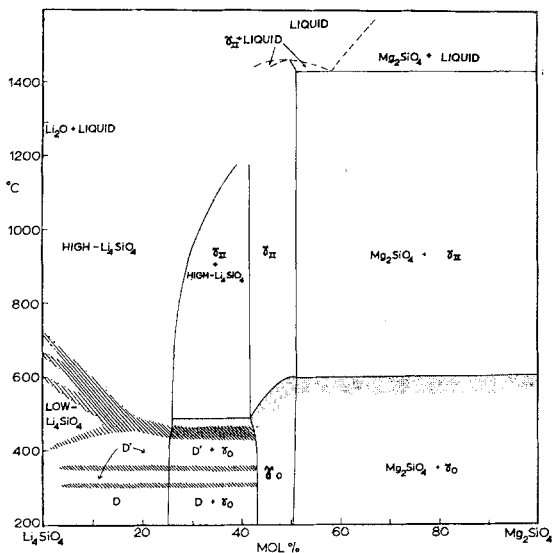


Figure 1 Phase equilibria in the system  $\text{Li}_4\text{SiO}_4\text{-Mg}_2\text{SiO}_4$ . Phase equilibria have not been studied in the lithium-rich portion of the system above 1150°C. The gradual inversion of high- $\text{Li}_4\text{SiO}_4$  to low- $\text{Li}_4\text{SiO}_4$  and, at higher magnesium contents to  $\text{D}'$  and  $\text{D}$  phases is discussed in more detail in the text; shaded zones separating the  $\text{D}$ ,  $\text{D}'$ , low- and high- $\text{Li}_4\text{SiO}_4$  phase fields represent regions of thermal activity as determined by DTA. All the crystalline phases except  $\text{Mg}_2\text{SiO}_4$  are solid solutions.

\*All percentages in this paper are in molM.

preparative methods were used: compositions between  $\text{Li}_4\text{SiO}_4$  and  $\text{Li}_2(\text{Zn, Mg})\text{SiO}_4$  had to be prepared from  $\text{Li}_4\text{SiO}_4$ ,  $\text{Mg}_2\text{SiO}_4$  and  $\text{Zn}_2\text{SiO}_4$ , rather than from  $\text{Li}_2\text{CO}_3$ ,  $\text{ZnO}$ ,  $\text{MgO}$  and  $\text{SiO}_2$ . Some of the subsolidus equilibria are apt to be sluggish, and additional experiments were done under hydrothermal conditions. In this technique, solid-phase reactants were put into gold foil envelopes. These were crimped shut, placed in a sleeve which also held a thermocouple, and the sleeve and thermocouple sealed into a pressurised reactor heated by an external furnace. Temperatures were read from the thermocouple; pressures were initially generated by an air-operated intensifier and read on bourdon-tube gauges. Water was used as the pressurising fluid. Pressures were generally maintained between 200 and 400 atmospheres. This was sufficiently high to speed up reactions which were very sluggish at normal pressures, yet not high enough either to induce new, high-pressure transformations, or to significantly shift the equilibrium temperature of a subsolidus reaction. No hydrate phases were formed in the hydrothermal reactions, nor were the samples subject to any serious leaching in runs of 24 to 48 h duration.

## 3. Results

### 3.1. The Binary System $\text{Li}_4\text{SiO}_4\text{-Mg}_2\text{SiO}_4$

Fig. 1 shows the phase equilibrium diagram which was constructed from the data. The liquidus was determined approximately by observing the melting temperatures of pelleted samples.  $\text{Mg}_2\text{SiO}_4$  forms a eutectic with another congruently melting compound, ideally  $\text{Li}_2\text{MgSiO}_4$ , at  $59 \pm 4$  mol%  $\text{Mg}_2\text{SiO}_4$  and  $1425 \pm 20^\circ\text{C}$ .  $\text{Li}_2\text{MgSiO}_4$  melts at  $1460 \pm 20^\circ\text{C}$ . The precise determination of the liquidus and solidus profiles was handicapped by the volatility of lithia. This volatility increases toward the lithium-rich end of the system, and it was not possible to determine melting relations in the range 0 to 45%  $\text{Mg}_2\text{SiO}_4$  with any accuracy.  $\text{Li}_4\text{SiO}_4$  itself is believed to melt incongruently to  $\text{Li}_2\text{O}$  and liquid [8]; the reported incongruent melting is shown schematically in fig. 1. At subsolidus temperatures, the volatility of lithium is not a serious problem (except in long runs at higher temperatures, as are required for high temperature X-ray (HXTR) photographs) and phase relations have been studied in detail.

$\text{Mg}_2\text{SiO}_4$  has the olivine structure at all temperatures. The solubility of  $\text{Li}$  in  $\text{Mg}_2\text{SiO}_4$

is very small, probably not exceeding 1% (as  $\text{Li}_4\text{SiO}_4$ ) at the solidus. A noteworthy feature of the phase relations is the appreciable range of stoichiometry of the  $\text{Li}_2\text{MgSiO}_4$  phase. At  $1100^\circ\text{C}$ , this range of homogeneous, single-phase formation extends from 41 to 51%  $\text{Mg}_2\text{SiO}_4$ . Thus the range of solid solution compositions lies largely displaced to the lithium-rich side of the ideal  $\text{Li}_2\text{MgSiO}_4$  composition. At  $600^\circ\text{C}$ , a  $\gamma_{\text{II}}\text{-Li}_2\text{MgSiO}_4$  composition inverts rapidly to a  $\gamma_0$ -type phase. The shaded transition zone in fig. 1 marking the  $\gamma_0 \rightleftharpoons \gamma_{\text{II}}$  inversion indicates that it extends over a range of temperatures. It is, of course, expected that in a normal first-order transition in a solid solution series, a two-phase loop will exist. In the present case, however, X-ray and DTA evidence shows that the transition extends over a 40 to  $50^\circ\text{C}$  temperature interval for all compositions, including  $\text{Li}_2\text{MgSiO}_4$  itself. In more lithia-rich compositions, the range of inversion temperatures drops markedly. The inversion is readily followed by DTA. The nomenclature of the polymorphs is, wherever possible, consistent with that assigned to the lithium zinc silicates. In the latter orthosilicate system, the  $\gamma_{\text{II}}$  phase inverts to the  $\gamma_0$  phase via an intermediate phase, designated " $\gamma_{\text{I}}$ " [7]. No evidence has been found for the existence of a  $\gamma_{\text{I}}\text{-Li}_2\text{MgSiO}_4$  solid solution at any composition. Although this introduces a gap in the nomenclature of the  $\text{Li}_2\text{MgSiO}_4$  polymorphs, the scheme retains the merit of indicating where isostructural relationships exist, which is important in systems such as these, where so many minor structural variants can occur.

$\text{Li}_4\text{SiO}_4$  itself forms an extensive range of magnesium-containing solid solutions. At temperatures up to  $1170^\circ\text{C}$ , a two-phase gap separates the fields of  $\text{Li}_4\text{SiO}_4$  and  $\text{Li}_2\text{MgSiO}_4$  solid solutions. At temperatures above  $\sim 800^\circ\text{C}$ , the width of this two-phase gap begins to contract markedly. The two-phase gap may persist up to the solidus, which is probably only slightly above  $1170^\circ\text{C}$ , but it is also possible that the two-phase gap closes over below the solidus, to give a range of solid solutions between  $\text{Li}_4\text{SiO}_4$  and  $\text{Li}_2\text{MgSiO}_4$  which are continuous, at least for some temperatures. It is difficult to obtain evidence on the phase behaviour of compositions in this range. In the time required for a high temperature X-ray, appreciable lithia loss occurs, as indicated by the formation of  $\text{Li}_2\text{SiO}_3$  in the sample. Brief heating, followed by quenching, produces new phases which are

believed to be metastable. On the other hand, quenching is necessary because solution and exsolution processes occur very rapidly, especially above about  $1000^\circ\text{C}$ . Many DTA patterns also show vague evidence of thermal activity beginning above about  $1000^\circ\text{C}$ . This may be associated with a non-quenchable transformation or with the onset of melting, either at the solidus in the binary system or at a "ternary"  $\text{Li}_2\text{O-MgO-SiO}_2$  invariant point. In summary, the equilibria are not known above  $1170^\circ\text{C}$ ; it is quite possible that  $\text{Li}_4\text{SiO}_4$  and  $\text{Li}_2\text{MgSiO}_4$  are completely miscible over a short range of temperatures just below the solidus.

$\text{Li}_4\text{SiO}_4$  itself is thermally active giving three reversible heat effects in the temperature range  $600$  to  $725^\circ\text{C}$ . These appear as small, but reasonably sharp effects on DTA. However, the inversions are not so clearly defined by HXTR. The entire range between  $600$  and  $725^\circ\text{C}$  is marked both by a rapid, but apparently continuous variation in the  $d$ -spacings and also by pronounced, but gradual, changes in the intensities of many of the reflections. The former effect is superimposed on the effects due to normal thermal expansion. It was concluded that these transformations are of the type loosely classified as "higher order". The effect of  $\text{Mg}^{2+}$  is to lower all three transformation temperatures and also, to cause each heat effect to spread over a wider range of temperatures, until by about 10%  $\text{Mg}_2\text{SiO}_4$  the separate effects have merged to give a single, very broad DTA signal. At the same time, the low- $\text{Li}_4\text{SiO}_4$  solid solutions are now able to undergo a new series of inversions, first to  $D'$  and then to  $D$  solid solutions. The nomenclature again shows the analogy with the phases observed in the  $\text{Li}_4\text{SiO}_4\text{-Zn}_2\text{SiO}_4$  system, although in that case the  $D$  and  $D'$  phases are metastable. The Mg-containing  $D$  and  $D'$  phases are readily distinguished from either high- or low- $\text{Li}_4\text{SiO}_4$  solid solutions by high-resolution X-ray powder photographs. The distinction is shown diagrammatically in fig. 2; powder data are also collected in table I. The  $D$  phase is probably a superstructure of  $\text{Li}_4\text{SiO}_4$  which arises by ordering of  $\text{Li}^+$  and  $\text{Mg}^{2+}$  ions. The development of  $D'$  and  $D$  from  $\text{Li}_4\text{SiO}_4$  solid solutions is sufficiently rapid to be followed by DTA. Several reversible heat effects are observed: one at  $300$  to  $320^\circ\text{C}$  is associated with the  $D \rightleftharpoons D'$  transformation. A smaller effect at  $340$  to  $360^\circ\text{C}$  is correlated with the onset of a progressive change in the  $D'$  phase

TABLE I X-ray powder diffraction data for lithium magnesium orthosilicates

$\gamma_{II}$		$\gamma_0$		lithia- $\gamma_0$		
$d(\text{\AA})$	I	$d(\text{\AA})$	I	$d(\text{\AA})$	I	$hkl$
*5.50	< 10	5.50	20	5.50	20	110
5.40	10	5.40	10	5.40	20	020
4.55	< 10	4.60	< 10	4.58	< 10	011
4.09	100	4.09	80	4.09	100	120
				4.08	20	
3.93	80	3.93	60	3.92	80	101
		3.90	20	3.90	20	
3.67	20	3.67	40	3.67	60	111, 021
3.66	10					
3.16	40	3.17	< 10	3.16	20	200, 121
		3.15 <sub>5</sub>	20	3.15	10	
3.10	< 10	3.10	20	3.10	20	130
2.90	20	2.90	10	2.90	10	031
2.72	100	2.71	80	2.71	100	220
2.66 <sub>5</sub>	60	2.66 <sub>5</sub>	60	2.68	40	201, 040
				2.67	80	
2.63 <sub>5</sub>	40	2.64	20	2.64	40	131
		2.62 <sub>5</sub>	20	2.63	40	
2.58	40	2.59 <sub>5</sub>	20	2.59	40	211
		2.57	20	2.57	40	
				2.56 <sub>5</sub>	40	
				2.52	40	
2.49 <sub>5</sub>	100	2.49 <sub>5</sub>	100	2.49 <sub>5</sub>	80	002
(a)		(a, g)		(b, g)		

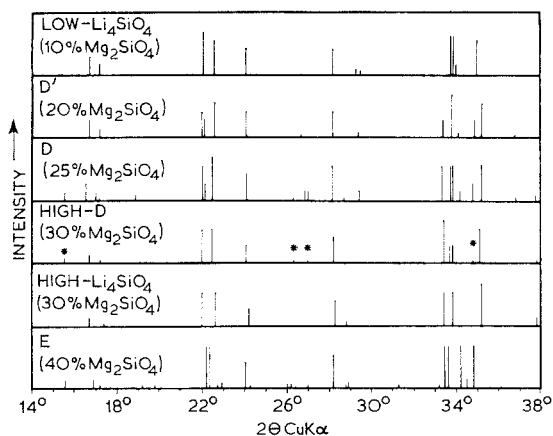


Figure 2 X-ray powder diffraction data at 25°C for some of the  $\text{Li}_4\text{SiO}_4\text{-Mg}_2\text{SiO}_4$  phases which are structurally related to  $\text{Li}_4\text{SiO}_4$ : the compositions of the solid solutions are in mole %. Powder data for high-D', which is also structurally similar, are not shown. Its pattern is identical with that of high-D, except that the reflections marked (\*) are absent for high-D'.

itself. This change continues up to 420 to 450°C. The D' phase, whose powder X-ray pattern now closely resembles that of a low- $\text{Li}_4\text{SiO}_4$  solid solution, may transform either to low- or high-

$\text{Li}_4\text{SiO}_4$  solid solution, depending upon its bulk composition. Further difficulties in the interpretation of results in the compositions containing 10 to 20%  $\text{Mg}_2\text{SiO}_4$  arise because the powder patterns of the low- and high- $\text{Li}_4\text{SiO}_4$  solid solutions become increasingly alike. The shaded regions in fig. 1 have been used to show how each of the higher-order transitions varies as a function of temperature and composition.

### 3.2. Non-Equilibrium Phase Transformations in the System $\text{Li}_4\text{SiO}_4\text{-Mg}_2\text{SiO}_4$

The lithium magnesium orthosilicates, like the lithium zinc orthosilicates, readily form metastable crystalline phases. The conditions for formation of each of the metastable phases are quite reproducible, but are sharply dependent on the bulk composition and phase composition of the starting materials, and on the nature of the thermal treatments used. Some typical conditions for producing the metastable phases are given in fig. 3. The four metastable phases have been designated high-D, high-D', E and lithia- $\gamma_0$ . In addition, a number of phases which appear on the equilibrium diagram at higher temperatures, can be quenched to ambient over certain compositional limits. These are also listed: for example, a range of high- $\text{Li}_4\text{SiO}_4$  solid solutions

TABLE I *contd.*

HIGH-D'		HIGH-D		D		D'		HIGH-Li <sub>4</sub> SiO <sub>4</sub> ss			E	
<i>d</i> (Å)	I	<i>d</i> (Å)	I	<i>d</i> (Å)	I	<i>d</i> (Å)	I	<i>d</i> (Å)	I	<i>hkl</i>	<i>d</i> (Å)	I
		5.70	10	5.70	20						7.4	< 10
5.30	40	5.30	20	5.35	40	5.30	40	5.30	20	001	5.70	20
5.20	20	5.15	10	5.20	20	5.15	20	5.10	10	100	5.25	20
				5.15	10						5.15	10
				4.70	20						4.62	< 10
4.06	80	4.04	80	4.04	80	4.04	60	4.04	80	011	4.48	< 10
				4.01	40	4.02	40				4.01	100
3.98	80	3.96	80	3.96	100	3.93	80	3.93	80	110	3.98	100
3.71	60	3.69	40	3.69	60	3.69	60	3.68	40	101	3.91	< 10
		3.39	10	3.39	< 10						3.88	10
				3.32	20	3.34	10				3.70	60
		3.30	10	3.30	20						3.66	< 10
3.16	60	3.16	60	3.17	80	3.16	60	3.16	60	111	3.42	10
3.12	10			3.11	10			3.10	10	020	3.40	10
				3.04	20	3.04	< 10				3.30	< 10
2.69	80	2.68	100	2.69	80	2.68	40	2.68	80	021	3.16	80
2.66	60	2.66	40	2.66	80	2.65	100	2.65	80	120, 002	3.10	< 10
2.65	60	2.65	40	2.65	20	2.63	10				3.09	10
				2.62	40	2.57	40				2.86	< 10
		2.57 <sub>5</sub>	20	2.58	80	2.55	80	2.55	100	200	2.70	< 10
2.56	100	2.55 <sub>5</sub>	80	2.55	(f)			(d)			2.68	100
(c)		(d)		(e)							2.66 <sub>5</sub>	100
											2.62	100
											2.60	20
											2.58	100
											2.52	< 10
											(c)	

## NOTES:

\*This line was absent at 700°C; It may be due to a small amount of  $\gamma_0$ . Solid solution compositions (mole % Mg<sub>2</sub>SiO<sub>4</sub>): (a) 50 (b) 41 (c) 40 (d) 30 (e) 25 (f) 20; (g) indexed on the basis of pseudo-orthorhombic symmetry. All data were obtained at 25°C. Intensities were estimated visually.

containing 20 to 35% Mg<sub>2</sub>SiO<sub>4</sub> may be quenched to ambient, although high-Li<sub>4</sub>SiO<sub>4</sub> itself cannot be quenched using the same cooling rate. The fast quench rates were achieved by dropping 20 to 50 mg samples, wrapped in platinum foil, into mercury. When an initial high-temperature treatment is required to develop the appropriate phase composition, 1170°C has been specified. This temperature is not necessarily fixed, but is used where possible to facilitate comparison between the effects of changing bulk compositions and thermal treatments.

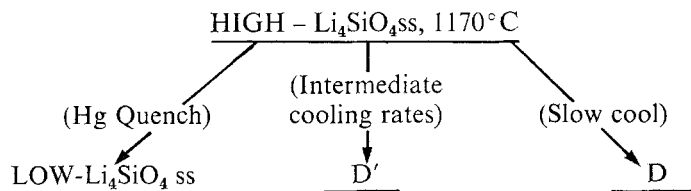
At 5 to 10% Mg<sub>2</sub>SiO<sub>4</sub>, the product obtained upon cooling varies with the speed of cooling: fast quenching gives a low-Li<sub>4</sub>SiO<sub>4</sub> solid solution; progressively slower cooling gives D' and D solid solutions respectively. At 30 to 35% Mg<sub>2</sub>SiO<sub>4</sub>, high-Li<sub>4</sub>SiO<sub>4</sub> solid solutions may be quenched to ambient. These are now metastable

with respect to the two-phase mixture ( $\gamma_0$  + D solid solutions). Upon reheating to 400°C no phase changes occur, but subsequent slow cooling of the solid solution to ambient yields a new phase, designated high-D. Comparison of the X-ray powder data for this phase with the patterns obtained for D, D' and Li<sub>4</sub>SiO<sub>4</sub> solid solutions (fig. 2) shows that while all have a close structural relation, the new phase is most closely related to the D phase, but its powder pattern is simpler; hence its designation as "high-D". Formation of high-D is dependent on being able to quench a homogeneous high-Li<sub>4</sub>SiO<sub>4</sub> without exsolution of  $\gamma$ -phases occurring. This exsolution is essential for formation of the equilibrium two-phase assemblages, but is sluggish at lower temperatures. The solid solution instead inverts to another homogeneous but metastable phase.

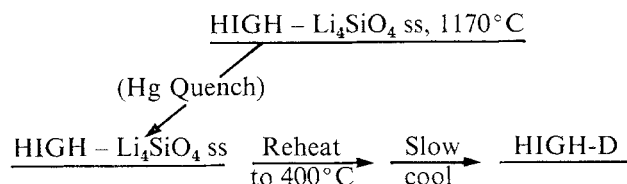
At 40% Mg<sub>2</sub>SiO<sub>4</sub>, a phase which is closely

COMPOSITION:—  
(mol %  $Mg_2SiO_4$ )

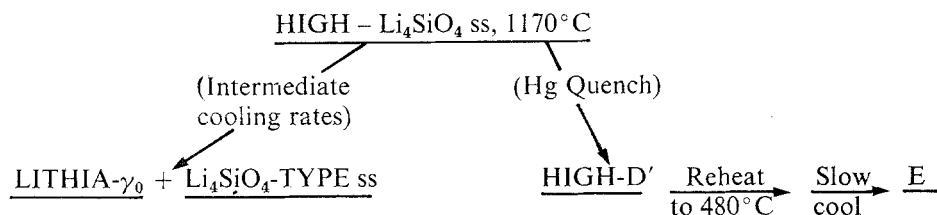
10 to 20



30 to 35



40



50

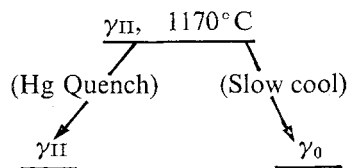


Figure 3 Some representative methods for the synthesis of metastable  $Li_4SiO_4$ - $Mg_2SiO_4$  phases. Solid solutions are abbreviated to ss.

related to high- $Li_4SiO_4$  solid solution can be quenched to ambient. Its powder pattern shows slight differences from those obtained in more lithia-rich compositions. For instance, in quenched high- $Li_4SiO_4$  solid solutions, the  $a$ -axis contracts regularly with increasing magnesium content. The 40% composition did not fit this trend. Instead, the powder pattern appeared to be intermediate between those of high-D and high- $Li_4SiO_4$  solid solutions; it has been designated "high-D'". Thus at 40%  $Mg_2SiO_4$ , a minor transformation probably occurs during quenching of high- $Li_4SiO_4$  solid solutions. It may be that high-D and high-D' are nothing more than metastable extensions of the D and D' phases respectively. However, powder patterns of the former pair are considerably simpler than those of the latter pair. Also, no patterns intermediate between the two types

(e.g. D and high-D, etc.) were ever obtained.

With slightly slower cooling rates some exsolution occurs giving a two-phase mixture. One of the phases is a  $Li_4SiO_4$ -type solid solution; the other is a distorted  $\gamma_0$  phase, designated "lithia- $\gamma_0$ ". Lithia- $\gamma_0$  occurs only at, or very close to, the lithia-rich limits of solid solution in the  $\gamma$ -type phases. It is probably metastable: for example, on prolonged heating at 300°C it transforms to a  $\gamma_0$  solid solution.

In the  $Li_4SiO_4$ - $Mg_2SiO_4$  system, the limits of the two-phase region ( $\gamma$ -type +  $Li_4SiO_4$ -type solid solutions) are accurate only to  $\pm 4\%$  in the temperature range 400 to 800°C. Because of the large number of phase assemblages possible, and the close similarity of many of the X-ray powder patterns, interpretation of the X-ray data from quenched samples was extremely difficult.

High- $Li_4SiO_4$  solid solutions containing 40%

$\text{Mg}_2\text{SiO}_4$  can also be used to prepare phase E. Rapid quenching from about  $1170^\circ\text{C}$  yields the high-D' phase. To obtain a quantitative yield of phase E, the high-D' is subsequently reheated to  $480^\circ\text{C}$  and slowly cooled to ambient. The conditions for formation of phase E are similar to those described for preparing high-D; a metastable solid solution yields a new metastable phase more readily than it exsolves. The reverse reaction (conversion of E to metastable high-D' solid solution) was followed by HTXR. The transformation took place in several steps which occurred between  $\sim 100$  and  $250^\circ\text{C}$ . None of the intermediate phases present at these steps were isolated, nor were further attempts made to characterise them.

At 50%  $\text{Mg}_2\text{SiO}_4$ , either  $\gamma_{\text{II}}$  or  $\gamma_0$  phase may be obtained at ambient, depending on the speed of cooling. No additional metastable phases could be produced in compositions containing  $> 50\%$   $\text{Mg}_2\text{SiO}_4$ .

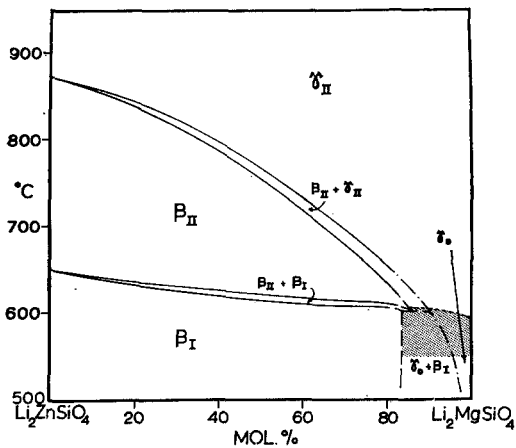


Figure 4 Phase equilibria at subsolidus temperatures on the join  $\text{Li}_2\text{ZnSiO}_4$ - $\text{Li}_2\text{MgSiO}_4$ . The gradual, higher-order transition between  $\gamma_0$  and  $\gamma_{\text{II}}$  solid solutions is shown by a stippled region.

### 3.3. The Ternary System $\text{Li}_4\text{SiO}_4$ - $\text{Mg}_2\text{SiO}_4$ - $\text{Zn}_2\text{SiO}_4$

#### 3.3.1. The Join $\text{Li}_2\text{MgSiO}_4$ - $\text{Li}_2\text{ZnSiO}_4$

Phase relationships on this join are shown in fig. 4. At subsolidus temperatures a continuous range of  $\gamma_{\text{II}}$  solid solutions sweeps across the diagram. With falling temperatures, this continues to  $\sim 870^\circ\text{C}$ ; at this temperature  $\gamma_{\text{II}}$   $\text{Li}_2\text{ZnSiO}_4$  inverts to the  $\beta_{\text{II}}$  phase. This inversion is sluggish at the  $\text{Li}_2\text{ZnSiO}_4$  composition. In static heating runs of a few days duration,  $\gamma_{\text{II}}$

converts completely to  $\beta_{\text{II}}$  at temperatures up to about  $750^\circ\text{C}$ ; on reheating, a  $\beta_{\text{II}} \rightarrow \gamma_{\text{II}}$  transition can be detected by DTA or HXTR. It occurs at  $\sim 870^\circ\text{C}$  over a broad range of heating rates; only at faster DTA heating rates does superheating occur. Thus the equilibrium inversion temperature is probably about  $870^\circ\text{C}$ . The effect of adding magnesium is two-fold; the  $\gamma_{\text{II}} \rightleftharpoons \beta_{\text{II}}$  inversion temperature falls and also, the conversion of  $\gamma_{\text{II}}$  to  $\beta_{\text{II}}$  becomes more sluggish. Thus, it becomes progressively more difficult to follow the inversion by static equilibration of samples in a dry atmosphere. It can, however, be readily followed under hydrothermal conditions. Inversion temperatures thus determined for the magnesium-rich compositions follow the trend which would be expected from this interpretation of the data obtained in "dry" runs. The two-phase region ( $\gamma_{\text{II}} + \beta_{\text{II}}$  solid solutions) is quite narrow, judged from HTXR photographs obtained on the heating cycle. The range of  $\beta$ -type solid solutions is not complete, but terminates between 80 and 100%  $\text{Li}_2\text{MgSiO}_4$ . Thus, fig. 4 shows schematically what occurs in this composition range. At 80%  $\text{Li}_2\text{MgSiO}_4$ , a  $\gamma$  solid solution converted completely to  $\beta$  in a hydrothermal run of 18 days duration at  $400^\circ\text{C}$ , but no  $\beta$  phase was ever obtained from  $\text{Li}_2\text{MgSiO}_4$  itself at either this or lower temperatures.

The  $\beta_{\text{I}} \rightleftharpoons \beta_{\text{II}}$  inversion is rapid, and can be followed reversibly by DTA. Addition of magnesium causes the inversion temperature to fall slowly from  $649^\circ\text{C}$  at the  $\text{Li}_2\text{ZnSiO}_4$  composition to  $611^\circ\text{C}$  at 80%  $\text{Li}_2\text{MgSiO}_4$ . The rate at which the  $\beta_{\text{II}} \rightleftharpoons \beta_{\text{I}}$  inversion is depressed by magnesium is not as rapid as that of the  $\beta_{\text{II}} \rightleftharpoons \gamma_{\text{II}}$  inversion, so the  $\beta_{\text{II}}$  field is diminished by adding magnesium. Eventually, a short range of compositions have a  $\beta_{\text{I}}$  solid solution which coexists with a  $\gamma$ -type solid solution; this is  $\gamma_0$ , but possibly includes  $\gamma_{\text{II}}$  over a short temperature interval: the gradual nature of the  $\gamma_0 \rightleftharpoons \gamma_{\text{II}}$  inversion in  $\text{Li}_2\text{MgSiO}_4$  has been mentioned earlier. It is probably coincidental that the peritectoid at which  $\beta_{\text{II}}$ ,  $\beta_{\text{I}}$  and  $\gamma$  solid solutions coexist also lies within the transitional zone between  $\gamma_0$  and  $\gamma_{\text{II}}$  solid solutions.

Although the  $\gamma_0 \rightleftharpoons \gamma_{\text{II}}$  inversion is stable over only a short composition range it may be followed metastably across the entire join, as  $\gamma_{\text{II}}$  solid solutions are readily undercooled with respect to the inversion to  $\beta$ . Fig. 5 shows the variation in  $\gamma_0 \rightleftharpoons \gamma_{\text{II}}$  inversion temperatures, as

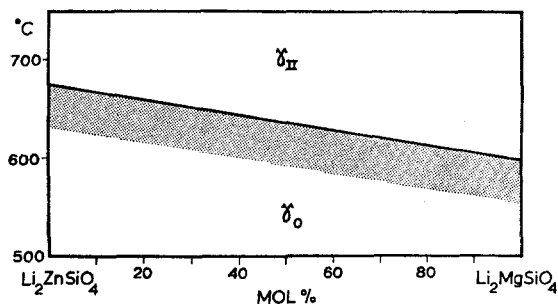


Figure 5 The  $\gamma_{II} \rightleftharpoons \gamma_0$  inversion in  $\text{Li}_2\text{ZnSiO}_4$ - $\text{Li}_2\text{MgSiO}_4$  solid solutions. The stippled region shows the approximate temperature interval of the transition. The stable portion of this inversion is also shown in fig. 4; however, in compositions from  $\text{Li}_2\text{ZnSiO}_4$  to about 90%  $\text{Li}_2\text{MgSiO}_4$ , the inversion is metastable.

determined by DTA. The reversible nature of the heat effects found by DTA, and their assignment to a  $\gamma_0 \rightleftharpoons \gamma_{II}$  inversion was confirmed by HTXR.

In a previous study [6] it was suggested that  $\beta_{II}$  need not invert directly to  $\beta_I$ - $\text{Li}_2\text{ZnSiO}_4$  on cooling, but that instead there might be a small temperature range in which another phase, designated  $\beta_{II}'$ , was stable. Its existence could only be demonstrated in static heating runs of a few days duration, where  $\beta_I$ - $\text{Li}_2\text{ZnSiO}_4$  converted first to  $\beta_{II}'$ , then to  $\beta_{II}$  on heating at progressively higher temperatures. Thus, the inversions  $\beta_{II} \rightleftharpoons \beta_{II}' \rightleftharpoons \beta_I$  were fully reversible in static runs; in dynamic runs, e.g. by HTXR,  $\beta_{II}'$  was only occasionally observed.

In the present study, the appearance of  $\beta_{II}'$  in some dynamic runs has been explained. If  $\beta_{II}'$ , prepared by static heating, is used as starting material it converts readily and reversibly to either  $\beta_{II}$  or  $\beta_I$  on heating and cooling respectively. On the other hand,  $\text{Li}_2\text{ZnSiO}_4$  which has never had the  $\beta_{II}'$  structure, tends to transform reversibly and directly from  $\beta_I$  to  $\beta_{II}$  without any intermediate  $\beta_{II}'$  phase being formed; thus  $\text{Li}_2\text{ZnSiO}_4$  crystals may retain a memory of their former existence as the  $\beta_{II}'$  phase.

Further evidence for a field of stability of  $\beta_{II}'$ - $\text{Li}_2\text{ZnSiO}_4$  has been obtained from hydrothermal experiments. A lithia-rich  $\gamma_0$  solid solution was used as the starting material. At 330 bars and 450°C, excess lithia was leached out during the run, leaving  $\beta_{II}'$ - $\text{Li}_2\text{ZnSiO}_4$  as the crystalline product. This  $\beta_{II}'$  could be heated by DTA to yield  $\beta_{II}$ , but unlike  $\beta_{II}'$  prepared by "dry" heating, the former transformed reversibly on

cooling only back to  $\beta_{II}'$ . The reversible  $\beta_{II} \rightleftharpoons \beta_{II}'$  inversion occurred at 642°C. On the other hand, hydrothermal synthesis at 450°C gave  $\beta_I'$  solid solutions at the  $\text{Li}_2(\text{Zn}_{0.7}\text{Mg}_{0.3})\text{SiO}_4$  composition, but at  $\text{Li}_2(\text{Zn}_{0.5}\text{Mg}_{0.5})\text{SiO}_4$  and  $\text{Li}_2(\text{Zn}_{0.2}\text{Mg}_{0.8})\text{SiO}_4$ , gave a  $\beta_I$  solid solution. By DTA the inversion of either  $\beta_I$ ,  $\beta_I'$  or  $\beta_{II}'$  to  $\beta_{II}$  occurred within a range of 10°C for any composition. Owing to the incomplete nature of the data regarding the individual stabilities of the  $\beta'$ -type phases, the  $\beta$ -phase field in fig. 4 has not been subdivided further. Some of the differences in the  $\beta_I$ ,  $\beta_I'$ ,  $\beta_{II}$  and  $\beta_{II}'$  powder patterns have been shown previously; the appearance of the patterns is virtually unchanged by substitution of magnesium for zinc.

Differences in some of the  $\gamma_0$ -phases following hydrothermal treatment were also observed. The composition  $\text{Li}_2(\text{Zn}_{0.2}\text{Mg}_{0.8})\text{SiO}_4$  was first reacted to give the  $\beta_I$  phase. On subsequent DTA heating, the  $\beta_I \rightarrow \beta_{II}$  and  $\beta_{II} \rightarrow \gamma_{II}$  inversions were found; on cooling, the  $\gamma_{II} \rightarrow \gamma_0$  inversion was observed, but at about 20° below the expected inversion temperature. Furthermore, the resulting  $\gamma_0$  powder pattern obtained at ambient had some lines which were abnormally diffuse and weakened, relative to ordinary  $\gamma_0$ . The diffuse lines had odd  $k$  indices (using orthorhombic indices for  $\gamma_0$ ). This product which may be a disordered  $\gamma_0$  phase, is designated  $\gamma_0'$ ; its pattern is shown, together with those of some other  $\gamma$ -type phases, in fig. 6.  $\gamma_0'$  could similarly be produced for other compositions, although it was never obtained for  $\text{Li}_2\text{ZnSiO}_4$  or  $\text{Li}_2\text{MgSiO}_4$ . Its inversion to  $\gamma_{II}$  was always lowered by 10 to 20°C, relative to the  $\gamma_0 \rightleftharpoons \gamma_{II}$  inversion temperature.

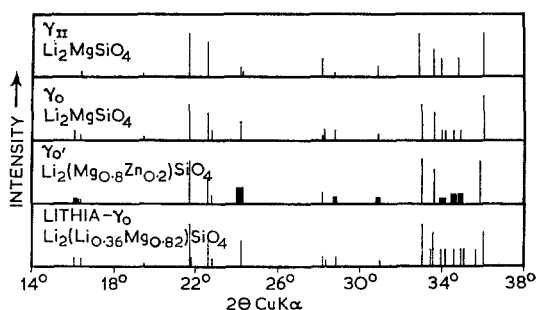


Figure 6 Powder X-ray diffraction data at 25°C for some of the  $\text{Li}_4\text{SiO}_4$ - $\text{Mg}_2\text{SiO}_4$ - $\text{Zn}_2\text{SiO}_4$  phases which are structurally related to  $\gamma_{II}$   $\text{Li}_2\text{MgSiO}_4$ . Diffuse reflections in the  $\gamma_0'$  phase are indicated by a thicker line.



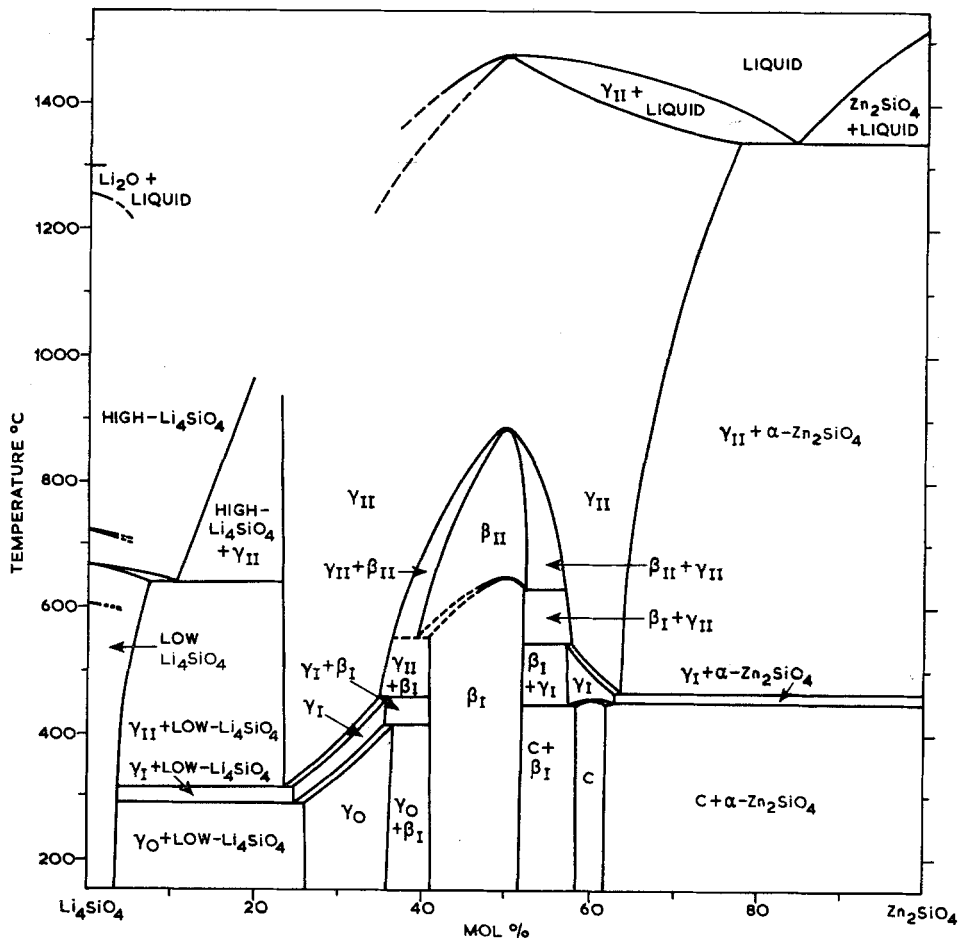


Figure 7 Phase equilibria in the system  $\text{Li}_4\text{SiO}_4\text{-Zn}_2\text{SiO}_4$ . The data are from reference [6].

### 3.3.2. The Ternary Phase Relations

The limiting binary systems have been studied in detail and are shown in figs. 1, 7 and 8. One minor correction to the data for the  $\text{Li}_4\text{SiO}_4\text{-Zn}_2\text{SiO}_4$  system should be noted. Re-examination of annealed  $\text{Li}_4\text{SiO}_4\text{-Zn}_2\text{SiO}_4$  compositions containing lithia-rich  $\gamma$  solid solutions, shows that a lithia- $\gamma_0$  solid solution is the equilibrium phase for compositions containing 25 to 35%  $\text{Zn}_2\text{SiO}_4$  below  $\sim 350^\circ\text{C}$ . Partly because of the difficulty of distinguishing a new, minor structural variant by X-ray powder methods alone, the significance of the line-splittings in the zinc-containing system had been overlooked. Thus in fig. 7, the equilibrium diagram for the system  $\text{Li}_4\text{SiO}_4\text{-Zn}_2\text{SiO}_4$ , the  $\gamma_0$  field is in fact, the lithia- $\gamma_0$  field, and  $\gamma_0$  is metastable at all compositions. By HTR, there is no intermediate  $\gamma_0$  phase in the

conversion lithia- $\gamma_0 \rightarrow \gamma_I \rightarrow \gamma_{II}$ . The field of  $\gamma_0$  in fig. 2 of [7] should be divided to include a field of lithia- $\gamma_0$  at its lithia-rich end. Also, the X-ray powder data given in Table 1A, [6] are for lithia- $\gamma_0$ . The  $\text{Mg}_2\text{SiO}_4\text{-Zn}_2\text{SiO}_4$  system has been studied [9, 10]; these results are shown in fig. 8. No compounds are formed;  $\text{Zn}_2\text{SiO}_4$  and  $\text{Mg}_2\text{SiO}_4$  are partially miscible.

Ternary isothermal sections have been studied at 1200, 900 and  $700^\circ\text{C}$ : these are shown as figs. 9, 10 and 11 respectively. At  $1200^\circ\text{C}$ , a broad range of  $\gamma_{II}$  solid solutions straddles the join  $\text{Li}_2\text{ZnSiO}_4\text{-Li}_2\text{MgSiO}_4$ . It has not been possible to study the Li-rich corner of the system at  $1200^\circ\text{C}$ . Hence the lithia-rich limits of the  $\gamma_{II}$  solid solutions are not known. However, the lower-lithia limits can be determined with more accuracy. The  $\gamma_{II}$  solid solution which is in

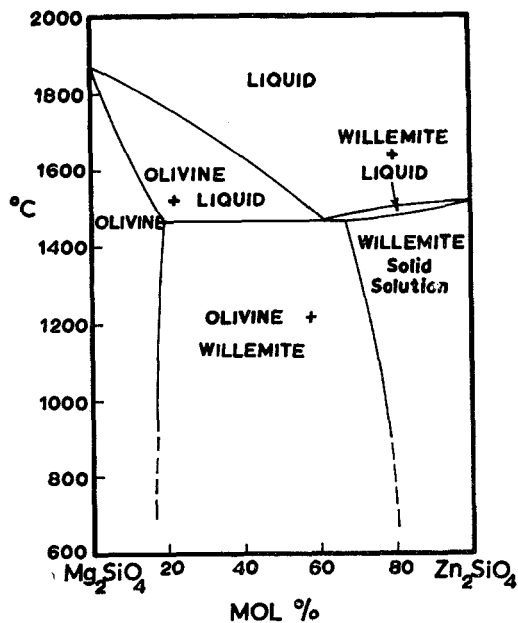


Figure 8 Phase equilibrium diagram for the system  $\text{Mg}_2\text{SiO}_4$ - $\text{Zn}_2\text{SiO}_4$ . The data are from references [9] and [10]; dashed lines represent the present author's extension of these data to 700°C. All the solid phases (olivine and willemite) are solid solutions.

equilibrium with both olivine and willemite solid solutions has the composition 51  $\text{Zn}_2\text{SiO}_4$ -28  $\text{Li}_4\text{SiO}_4$ -21  $\text{Mg}_2\text{SiO}_4$ . Addition of more magnesium causes a rapid contraction in the extent of the  $\gamma_{\text{II}}$  solid solution field. The effect of  $\text{Mg}^{2+}$ - $\text{Zn}^{2+}$  substitution on the appearance of the  $\gamma_{\text{II}}$  powder pattern is very small and the  $\text{Li}^+(\text{Mg}^{2+} + \text{Zn}^{2+})$  ratio of the solid solutions can be estimated from the X-ray powder patterns by simply using data collected for solid solutions on the  $\text{Li}_4\text{SiO}_4$ - $\text{Zn}_2\text{SiO}_4$  edge. The ternary limits of solid solution thus have to be estimated partly from the presence or absence of a second or third phase. The method is sensitive because  $\text{Mg}_2\text{SiO}_4$  and  $\text{Zn}_2\text{SiO}_4$  can be detected readily by X-rays. No ternary solid solution of  $\text{Li}_4\text{SiO}_4$  in either willemite or olivine solid solution was detected.

The positions of tie lines within the two-phase regions have not been determined accurately in this or other isothermal sections, but the limiting tie lines – for example, those which form the three-phase triangle (olivine + willemite +  $\gamma_{\text{II}}$  solid solutions) (fig. 9) – were determined accurately. These are reasonably regular, so that the other tie lines are also presumed to be regular.

At 900°C, (fig. 10) studies have been extended to the entire range of ternary compositions. The extent of the field of homogeneous  $\gamma_{\text{II}}$  solid solutions has contracted markedly, as compared to its extent at 1200°C; for example, the  $\gamma_{\text{II}}$  solid solution in equilibrium with both olivine and willemite solid solutions now lies at 52  $\text{Zn}_2\text{SiO}_4$ -33

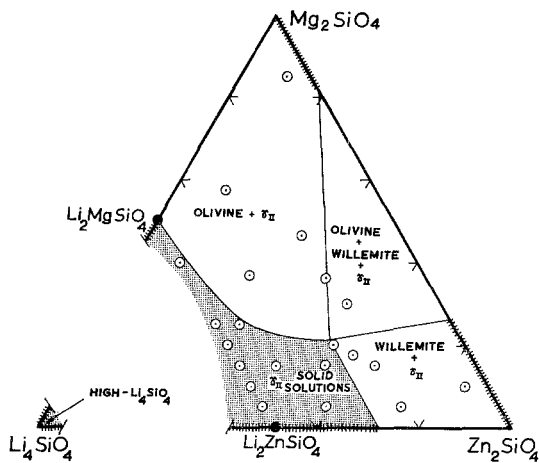


Figure 9 Phase equilibria in the system  $\text{Li}_4\text{SiO}_4$ - $\text{Mg}_2\text{SiO}_4$ - $\text{Zn}_2\text{SiO}_4$ ; the 1200°C isothermal section. Compositions studied are shown by small open circles. Ranges of binary solid solutions are shown by cross-hatched lines and ranges of ternary solid solutions by stippled areas. All the crystalline phases are thus solid solutions. Phase relations were not studied in the lithia-rich region; solidus temperatures may be below 1200°C.

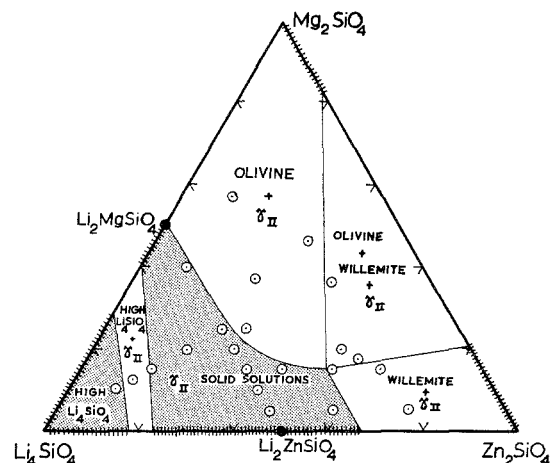


Figure 10 Phase equilibria in the system  $\text{Li}_4\text{SiO}_4$ - $\text{Mg}_2\text{SiO}_4$ - $\text{Zn}_2\text{SiO}_4$ ; the 900°C isothermal section. Other symbols are as in fig. 9.

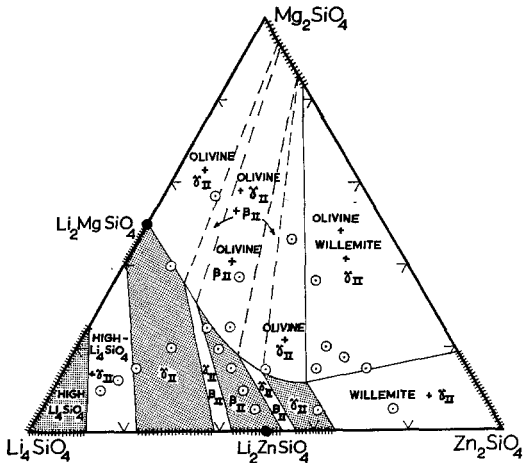


Figure 11 Phase equilibria in the system  $\text{Li}_4\text{SiO}_4\text{-Mg}_2\text{SiO}_4\text{-Zn}_2\text{SiO}_4$ : the  $700^\circ\text{C}$  isothermal section. Other symbols are as in fig. 9. Phase relations on the  $\text{Li}_2\text{ZnSiO}_4\text{-Li}_2\text{MgSiO}_4$  join are shown in fig. 4. The repetition of the same one- and two-phase fields (e.g. fields of  $\gamma_{\text{II}}$ , or  $\gamma_{\text{II}} + \beta_{\text{II}}$  solid solutions) at different places on any one isothermal section is a most unusual feature of this and other isothermal sections taken at temperatures below about  $870^\circ\text{C}$ .

$\text{Li}_4\text{SiO}_4\text{-15 Mg}_2\text{SiO}_4$ . The contours of the magnesium-rich limit of the  $\gamma_{\text{II}}$  phase field are similar at both 900 and  $1200^\circ\text{C}$ . At  $900^\circ\text{C}$ , high- $\text{Li}_4\text{SiO}_4$  and  $\gamma_{\text{II}}$  solid solutions are separated by a two-phase gap. The shape of the intervening two-phase region is not known.

At  $700^\circ\text{C}$  (fig. 11), the  $\gamma_{\text{II}}$  solid solution field is now disrupted by the conversion of  $\text{Li}_2\text{ZnSiO}_4$  and a range of ternary compositions to the  $\beta_{\text{II}}$  phase.  $\text{Li}_2\text{MgSiO}_4$  itself does not form a  $\beta$ -type phase at any temperature and this is reflected in the shape and direction of the field of  $\beta_{\text{II}}$  solid solutions. Another novel feature of this isothermal section is the appearance of *two* separate fields of  $\gamma_{\text{II}}$  solid solutions. This is caused by the increasing thermal stability of the  $\beta$ -type phase, at or close to the  $\text{Li}_2\text{ZnSiO}_4$  composition; alternatively, it may be easier to picture it as due to the decreasing stability of the  $\gamma$ -type solid solution as the  $\text{Li}_2\text{ZnSiO}_4$  composition is approached from either direction. The contraction of the  $\gamma$ - and  $\beta$ -solid solution fields (taking both collectively), continues with falling tempera-

ture. Thus at  $700^\circ\text{C}$ , the  $\gamma_{\text{II}}$  solid solution which is in equilibrium with both olivine and willemite solid solutions lies at 53  $\text{Zn}_2\text{SiO}_4\text{-36 Li}_4\text{SiO}_4\text{-11 Mg}_2\text{SiO}_4$ . The compositions of the olivine and willemite solid solutions coexisting at  $700^\circ\text{C}$  were estimated by extending the data in fig. 8; inasmuch as the solubilities change only slightly with temperature in this range, this is probably valid. Direct reaction of olivine and willemite to give the equilibrium assemblage is only possible under hydrothermal conditions at  $700^\circ\text{C}$ . As a consequence of the partial inversion of some  $\gamma_{\text{II}}$  solid solutions to  $\beta_{\text{II}}$  solid solutions, the field of (olivine +  $\gamma_{\text{II}}$  solid solutions) is broken up into a series of two- and three-phase regions. The two-phase gap separating  $\gamma_{\text{II}}$  and high- $\text{Li}_4\text{SiO}_4$  solid solutions has expanded and become more asymmetric due to the rapidly decreasing solubility of  $\text{Li}_2\text{ZnSiO}_4$  in  $\text{Li}_4\text{SiO}_4$  with falling temperatures.

For isothermal sections below  $700^\circ\text{C}$ , the size and shape of the various fields should follow the trends already established. New fields will appear – for example, a field of  $\gamma_0$  solid solutions will appear below  $670^\circ\text{C}$  – while other fields present at  $700^\circ\text{C}$ , e.g. that of  $\beta_{\text{II}}$  solid solutions, will disappear.

### Acknowledgement

A.R.W. has a University studentship from the Robbie, Japp and Coutts Funds. The Science Research Council has provided funds for equipment and materials.

### References

1. F. P. GLASSER, *Phys. Chem. Glasses* **8** (1967) 224.
2. A. R. WEST and F. P. GLASSER, *Mat. Res. Bull.* **5** (1970) 837.
3. J. WILLIAMSON and F. P. GLASSER, *Phys. Chem. Glasses* **5** (1964) 52.
4. P. W. MCMILLAN, S. V. PHILLIPS, and G. PARTRIDGE, *J. Mater. Sci.* **1** (1966) 269.
5. I. M. STEWART, I. BROUGH, and L. GREEN, *ibid* **2** (1967) 63.
6. A. R. WEST and F. P. GLASSER, *ibid* **5** (1970) 557.
7. *Idem*, *ibid* **5** (1970) 676.
8. F. C. KRACEK, *J. Phys. Chem.* **34** (1930) 2641.
9. J. F. SARVER and F. A. HUMMEL, *J. Amer. Ceram. Soc.* **45** (1962) 304.
10. E. R. SEGNET and A. E. HOLLAND, *ibid* **48** (1965) 409.

Received 14 December 1970 and accepted 24 March 1971.